Incommensurate Transition-Metal Dichalcogenides via Mechanochemical Reshuffling of Binary Precursors

Ihor Z. Hlova,[1]‡ Prashant Singh,[1]‡ Serhiy Z. Malynych,[2] Roman V. Gamernyk,[3] Oleksandr Dolotko,[1] Vitalij K. Pecharsky,[1,4] Duane D. Johnson,[1,4] Raymundo Arroyave,[5] Arjun K. Pathak,[6] Viktor P. Balema[1]**

[1]Ames Laboratory, U.S. Department of Energy, Iowa State University, Ames, IA, 50011-2416, USA
[2]Hetman Petro Sahaidachnyi National Army Academy, Lviv, 79026, Ukraine
[3]Ivan Franko National University of Lviv, Lviv, 79005, Ukraine
[4]Department of Materials Science and Engineering, Iowa State University, Ames, IA, 50011-1096, USA
[5]Department of Materials Science & Engineering, Texas A&M University, College Station, TX, 77843, USA
[6]Department of Physics, SUNY Buffalo State, Buffalo, NY, 14222, USA

Figures referenced in the text.

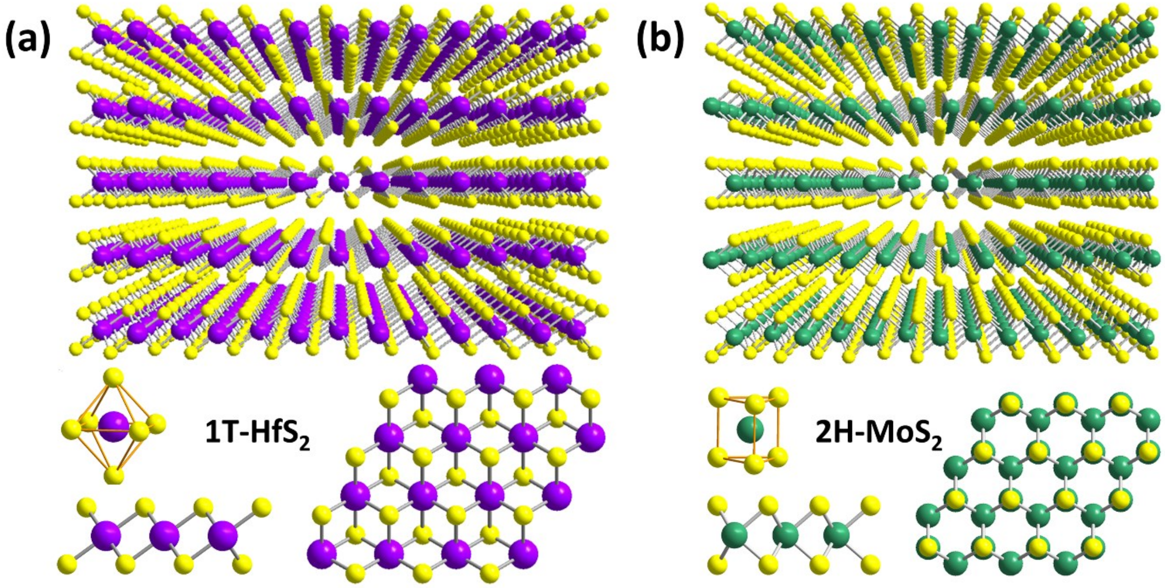

Figure S1. Perspective views of layered van der Waals transition metal dichalcogenides together with the coordination polyhedra of transition metal atoms and different projections of the individual layers (a) 1T-HfS$_2$ and (b) 2H-MoS$_2$. Hf and Mo are depicted, respectively, as violet and green, and sulfur as yellow spheres.

Additional experimental details

Materials:

Ultra-high purity Ar (Matheson, 99.999%), ultra-high purity He (Matheson, 99.999%), MoS_2 (Alfa Aesar, 99% purity), Hf (Alfa Aesar, 99.6%), Mo (99.9% purity) and S (Alfa Aesar, 99.998% purity). HfS_2 was prepared in-house from elements.

Synthesis of HfS_2:

The precursor HfS_2 was prepared by ball milling of a stoichiometric mixture of hafnium and sulfur (5% excess) for 8 hours in a shaker mill in silicon nitride vial and then sealed in a quartz ampule under 0.75 bar pressure of ultra-high purity helium and annealed for 3 days at 1000 °C. The powder X-ray diffraction (XRD) analysis of the obtained material confirmed the formation of the pure HfS_2 phase (Figure S2).

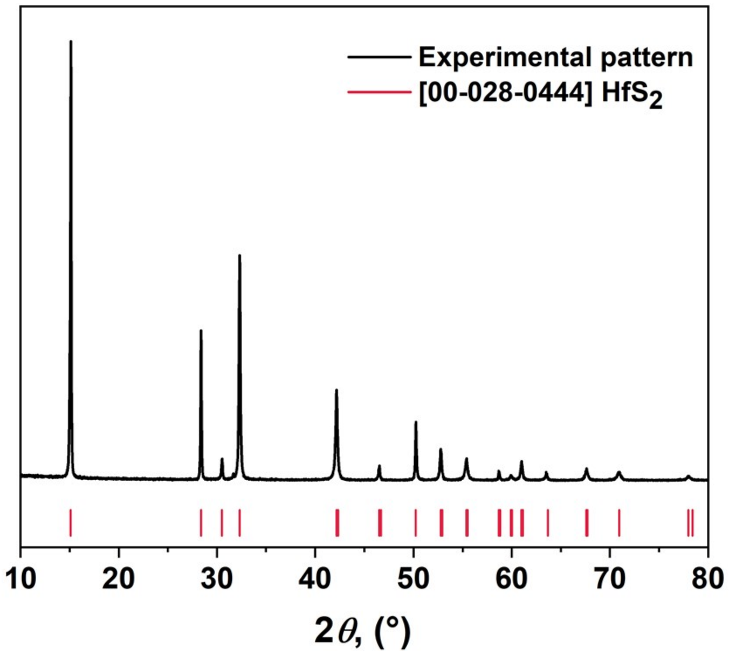

Figure S2. The powder XRD pattern of HfS_2 prepared from the elements. Vertical bars at the bottom of the chart correspond to calculated Bragg peak positions of HfS_2.

Powder X-ray Diffraction (XRD):

The structure-factor independent (Le Bail) fits were performed to determine lattice parameters of the constituent phases (Figure S3). MoS_2 and HfS_2 ($P6_3/mmc$ and P-$3m1$) were treated as two separate phases, each contributing their own set of Bragg reflections to the overall powder XRD pattern.

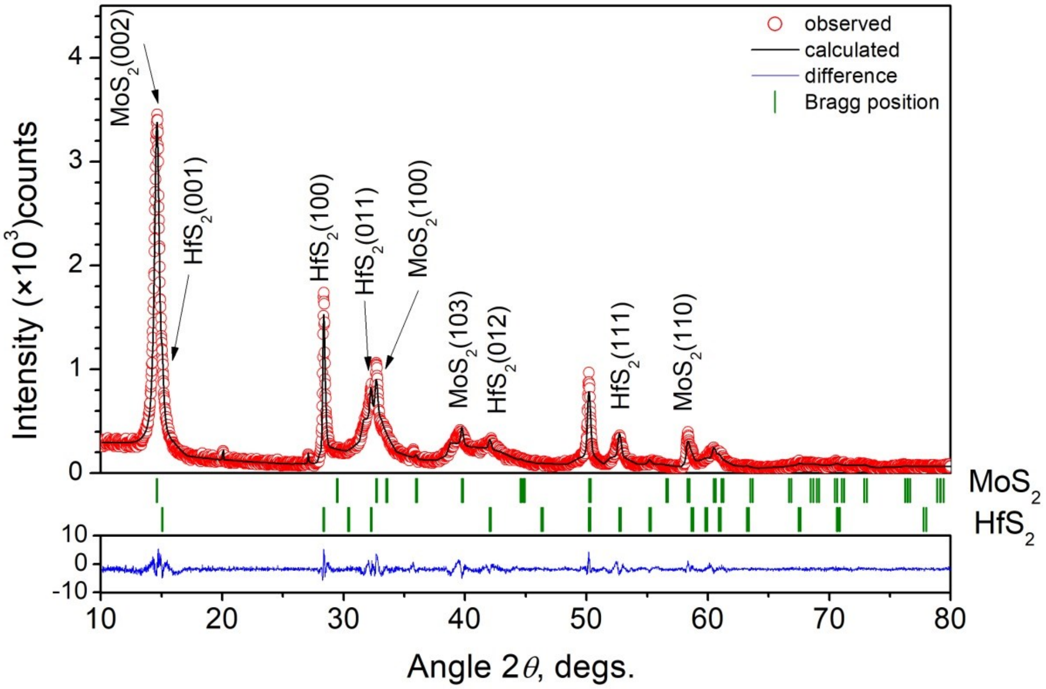

Figure S3. Example of the Le Bail fit of powder XRD pattern of a 50:50 MoS_2-HfS_2 heterostructure. Vertical bars at the bottom of the chart represent calculated positions of the Bragg peaks of MoS_2 and HfS_2 as marked. Indices are shown for easily distinguishable Bragg reflections of the two phases.

Band gap measurements

Sample preparation for optical and photoconductivity measurements

Conventional microscope glass was cut into ~10×10 mm^2 pieces. Droplets of silver paste were deposited onto the glass surface to make electrical contacts. Before the paste hardened, thin copper wires were introduced into the droplets, making electrical measurements convenient.

Suspensions of powdered samples in isopropanol were deposited on the glass slides. After drying at ambient conditions, thin films adhering to the surfaces of the glass slides, making direct connections with the silver paste droplets were obtained. The films are non-transparent and appear as coal-black layers with thickness between 1 and 3 μm as measured using an optical profilometer. Optimal film thickness can slightly vary since too thin films fall under percolation limits and are poorly conducting, while too thick coatings are completely opaque.

Photoconductivity measurements

Stabilized power source was used for photoelectrical studies. Photocurrent was registered by electrometer equipped with ADC CS5522 (Cirrus Logic, Inc.) analog-to-digital converter. All photocurrent spectra were normalized to the same number of incident photons employing non-selective detector of electromagnetic radiation. In crystalline semiconductors photoconductivity plotted as a function of energy usually indicates the smallest direct energy gap. However, if the excitons exist in the material, the exciton binding energy should be added to the photon energy in order to obtain the gap. Photoconductivity measurements of powder samples is a challenge since the electrical contact between adjacent granules (crystallites) as well as their surface states strongly affect the overall conductivity.

The sample was placed into cryostat when desired. The cryostat allows controlling the temperature within 78-300 K range with 0.1 K accuracy.

The optical band gap was determined using the following relation [1]:

$$\alpha = \frac{B\left(h\nu - E_g\right)^n}{h\nu},$$

where $h\nu$ is the incident photon energy, α is the absorption coefficient, B is a materials dependent constant, and E_g is the optical band gap.

The usual method of determining E_g involves plotting $(\alpha h\nu)^{1/n}$ vs. $h\nu$ (Tauc plot) [2, 3]. By extrapolating the linear portion of the $(\alpha h\nu)^{1/n}$ vs. $h\nu$ plot to $\alpha = 0$, one can estimate the band gap from the absorption curve.

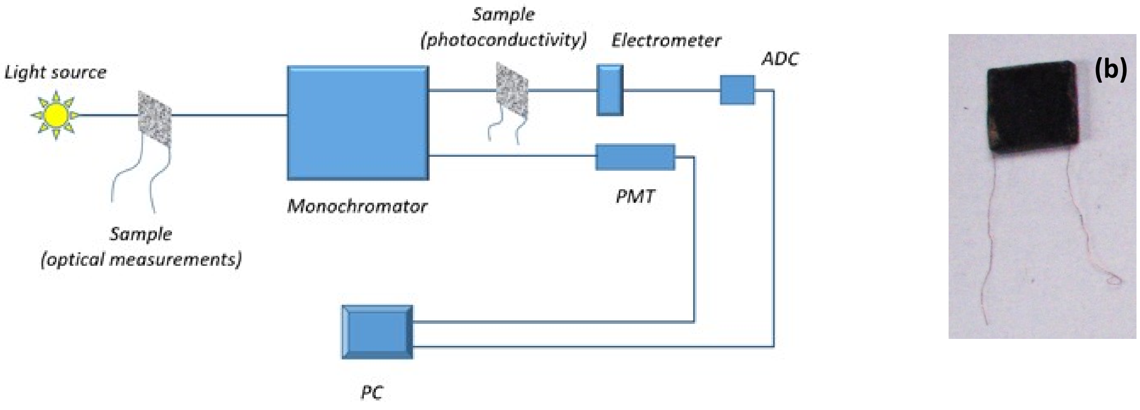

Figure S4. (a) Experimental setup for photoconductivity measurements (ADC is an analog-to-digital converter, PMT is a photomultiplier tube, PC is personal computer) and (b) a photograph of a typical sample with the 2 μm thick material layer.

Depending on whether the transition is direct allowed, direct forbidden, indirect allowed or indirect forbidden, *n* takes the value 1/2, 3/2, 2 or 3, respectively.

The best fits in this study were observed for $n = 2$ or $(\alpha h\nu)^{1/2}$, which indicates the indirect allowed transition. Note that both optical and photoconductivity measurements yield practically the same values of E_g for ($Hf_{0.5}Mo_{0.5}S_2$) $E_g = 0.96$ eV and ($Mo_{0.45}W_{0.45}Hf_{0.1}S_2$) $E_g = 1.03$ eV samples.

Density Functional Theory (DFT) calculations

Effect of Se doping on band-structure $(Mo_{0.5}W_{0.5})S_2$: Doping $(Mo_{0.5}W_{0.5})S_2$ with Se at S-site has a very weak effect on electronic structure that reduces the bandgap of $(Mo_{0.5}W_{0.5})(S_{0.5}Se_{0.5})_2$ by 0.17 eV compared to $(Mo_{0.5}W_{0.5})S_2$. However, we do not observe any significant change in the shape of band-structure or partial DOS, see Figure 5 in the main text. The charge density plots in Figure 5 are almost identical. We believe that this comes from the fact that both (Mo, W) and (S, Se) are iso-electronic. To understand the possible reason for the weak effect of Se doping on band gap, we look at the atomic sizes of S and Se, where the atomic radius of Se (1.17 Å) is 11% bigger than that of S (1.04 Å). After the structural relaxation of $(Mo_{0.5}W_{0.5})(S_{0.5}Se_{0.5})_2$, we found that the average bond-length for Se-doped case is 2.481 Å, which is approximately 2.6 percent bigger than $(Mo_{0.5}W_{0.5})S_2$. The average bond-length for $(Mo_{0.5}W_{0.5})S_2$ is 2.416 Å. We also notice that major bong-length change occurs whenever Se sits around Mo, whereas Se shows no significant change in W-Se/W-S bond-length. Increased Mo-S/Mo-Se bond-length weakens the chemical bonding, i.e., delocalizes the bonding states, which leads to a small change in the band gap.

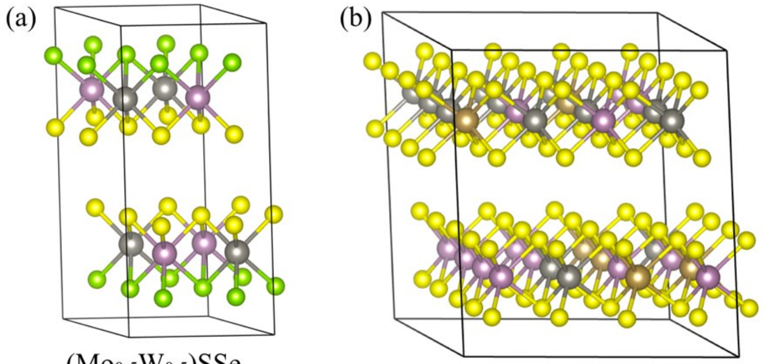

$(Mo_{0.5}W_{0.5})SSe$

$(Mo_{0.4}W_{0.4}Ta_{0.2})S_2$

Figure S5. (a) In Fig. 5 (main text), a 2x2x2 supercell was used to model W-disorder on Mo site with 24 atom cell (Mo=4, W=4, S=16; and Mo=4, W=4, S=8, Se=8) atom per cell. (b) In Fig. 6 (main text), a 4x4x2 supercell was used to model the 0.4 (Mo):0.4 (W):0.2 (Ta) disorder with 96 atom per cell (Mo=13, W=13, Ta=6, S=64).

Registry index quantifying the degree of interlayer commensurability, has been included in the phase-stability and band-structure of ($2H-MoS_2$:$1T-HfS_2$) supercell through full (volume and atomic) relaxation in DFT calculations.

Observation on reproducibility and heterostructure constitution

Each sample was synthesized at least twice, and the results were fully reproducible (see Fig. S6 as an example). STEM experiments were performed on at least 10 different particles per each sample. All of the examined particles contained mixed layers similar to those shown in Fig. 1 and 2 in the main text. We did not detect starting materials as separate components of the powders formed. Slabs typically contained between 3 and 12 single phase HfS_2 and MoS_2 layers which agrees well with the model described in the main text. Individual particles of heterostructured materials ranged from 50 nm to ~1 μm and consisted of ~30 to 100+ layers stacks. Particle size of starting materials before ball milling did not exceed 2 μm.

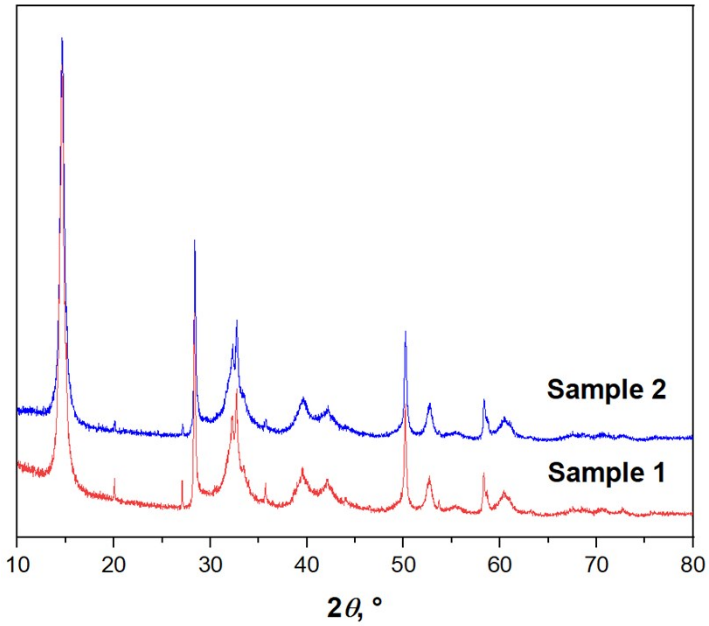

Figure S6. Powder XRD patterns of two separate samples prepared from equimolar mixtures of HfS_2 and MoS_2 ball-milled for 30 hours in a planetary mill and subsequently annealed at 1000°C for 72 hours.

REFERENCES

1. Mott, N. F.; Davis, E. A. Electronic Processes in Non-Crystalline Materials. Clarendon Press: Oxford, **1979**.

2. Ghobadi, N. Band Gap Determination Using Absorption Spectrum Fitting Procedure. *Int. Nano Lett.* **2013**, *3*, 2.

3. Suram, S. K.; Newhouse, P. F.; Gregoire, J. M. High Throughput Light Absorber Discovery, Part 1: An Algorithm for Automated Tauc Analysis. *ACS Comb. Sci.* **2016**, *18*, 673−681.